J. Fluid Mech. (1972), *vol.* 55, *part* 2, *pp.* 301–310
Printed in Great Britain

An experimental and analytical investigation of angular momentum exchange in a rotating fluid

By M. DUNST

Meteorologisches Institut, Universität Hamburg

(Received 3 March 1972)

Stimulated by considerations of the shear structure of the tropospheric jet stream, we have performed a series of experiments in a rotating vessel (using water, barotropic model) to study the angular momentum exchange in a rotating fluid. In the experiments, a cylinder was fitted in the centre of a cylindrical vessel (of large diameter) rotating around the vertical axis and could rotate independently around the same axis in both directions. The experimental results are as follows. (i) For constant relative rotation with the inner cylinder acting as a source (sink) of angular momentum, the momentum exchange becomes stationary, the bottom of the vessel being a sink (source) of momentum. The zone for this exchange is confined to a relatively small area around the inner cylinder. Beyond this zone, the 'friction' zone, no relative motion can be observed. Essentially the radial extent b of the 'friction' zone depends on the dimensionless parameter $\epsilon = \Delta\omega/\omega$ ($\Delta\omega$ = relative rotation rate of inner cylinder, ω = rotation rate of vessel): $b(|\epsilon|) > b(-|\epsilon|)$. (ii) The velocity field shows a strong tendency to be two-dimensional, the radial and vertical components being about one to two orders of magnitude smaller than the zonal component, whose absolute value decreases monotonically from the inner cylinder to the outer limit of the 'friction' zone. Elementary analytical considerations indicate that inertial stability seems to be the key for the understanding of these results.

1. Introduction

A cross-section through the high tropospheric jet reveals that on the cyclonic side the wind decrease is more pronounced than on the anticyclonic side. The anticyclonic profile can to a fair degree be approximated by vanishing absolute vorticity, $\xi_a = 0$ (process of lateral mixing), whereas the cyclonic profile may be characterized by $\xi_a = K$, where K is a positive constant (Rossby 1947; Bannon 1952; Reiter 1961). To gain more insight into this phenomenon, which can roughly be explained through considerations of inertial stability, a series of experiments in a rotating vessel filled with water has been performed using the following arrangement. In the centre of a cylindrical vessel rotating around the vertical axis a second cylinder was installed and could rotate independently around the same axis in both directions, thus inducing either cyclonic or anticyclonic motions of the water relative to the rotating vessel. The shear zones could be made visible by coloured agents.

Compared with atmospheric conditions our experiments are subjected to some simplifications. For instance there is no density or temperature gradient, i.e. our model is barotropic; moreover, the geometrical and dynamical similarity conditions have to be considered. On the other hand such experiments can throw some light on the dynamical problem of lateral mixing in the jet stream because the process of horizontal exchange of angular momentum and the influence of rotation upon this process can be studied systematically without being complicated by baroclinic effects.

A first series of experiments (Dunst 1967) yielded essentially the following results. The exchange of angular momentum reaches a steady state, in which the inner cylinder produces as much angular momentum as is transported through the bottom of the vessel. The zone in which this exchange takes place is restricted to a relatively small area around the inner cylinder. Only in this well-defined zone, which we call the friction zone, does there exist a relative motion; beyond this no relative motion can be observed. Moreover, the radial extent of the friction zone depends upon the absolute value and the sign of shearing vorticity or, more precisely, of the dimensionless parameter $\Delta\omega/\omega$, where $\Delta\omega$ is defined by $\Delta\omega = \omega' - \omega$, ω' denoting the angular velocity of the inner cylinder and ω that of the vessel. For $\Delta\omega < 0$ (cyclonic shearing vorticity) the radial extent of the friction zone is smaller than for $\Delta\omega > 0$ (anticyclonic shearing vorticity). It is only in the case $\omega = 0$ that no sharply bounded friction zone is found at all; in fact, in the whole vessel we observe a steady three-dimensional motion.

These results (except for the case $\omega = 0$) are in rough agreement with observations concerning the situation in the tropospheric jet stream. Model experiments like those described above seem to be quite well suited to give more insight into the shear structure and the problem of turbulent exchange of angular momentum. Therefore some more experiments have been performed, the essential results of which will be given in detail below.

2. The model apparatus

The main part of the model (see figure 1, plate 1) is the cylindrical Plexiglas vessel Z_a, which rotates around the vertical axis with angular velocity $\omega\,\mathrm{s}^{-1}$ and has diameter $2d = 100$ cm and height 50 cm. ω satisfies the relation $\omega = (2\pi/60)\,n_1$, where n_1 is measured revolutions per minute; in our experiments $0 \leqslant n_1 \leqslant 60$. The angular velocity ω' of the smaller inner cylinder Z_i satisfies $\omega' = (2\pi/60)\,n_2$, with $0 \leqslant n_2 \leqslant 100$ r.p.m. The rotation relative to the vessel (system of reference) is given by $\Delta\omega = \omega' - \omega = (2\pi/60)\,(n_2 - n_1)$ (see figure 2). Normally the vessel is filled with water to a height of 20 cm, with a free surface, but for certain experiments we used a rigid upper boundary: a lid fixed to the vessel. The flow in the vessel can be made visible using different coloured agents, which diffuse into the water through a very small slit (0·2 cm wide) at the ground between the inner cylinder and the bottom. Observations are made from the side and from above. The field of motion relative to the vessel can be photographed by a rotating camera attached to the vessel.

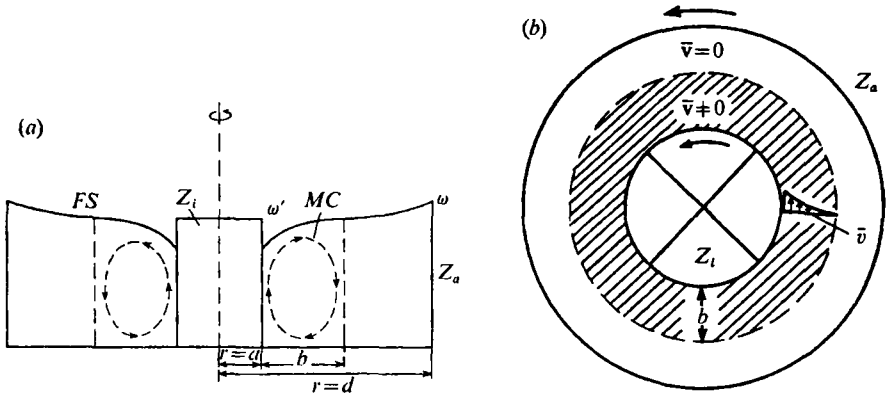

FIGURE 2. (*a*) Cross-section of experimental arrangement (schematic). Z_a, cylindrical vessel with angular velocity ω and diameter $2d$; Z_i, inner cylinder with angular velocity ω' and diameter $2a$; b, radial extent of the 'friction' zone; *MC*, meridional circulation, for $\epsilon > 0$; *FS*, free surface. (*b*) View of experimental arrangement (schematic). $\bar{\mathbf{v}}$ = mean velocity vector, $\bar{v}$ = zonal component of $\bar{\mathbf{v}}$.

3. The experiments

A characteristic quantity of the experiments (see figure 2) is the radial extent b of the so-called friction zone. The friction zone is defined as the region in which a relative motion induced by the inner cylinder exists. In general the friction zone occupies only a narrow area, and beyond this no relative motion can be observed. Essentially, the experiments were performed as follows. The initial state is the solid-body rotation of the water, then, after the relative rotation of the inner cylinder has been started, a turbulent flux of angular momentum sets in, and the friction zone gradually develops until, after some minutes, a steady state is reached. By diffusing dye the individual phases of the experiment can be followed.

The most important experimental parameter is the ratio $\epsilon = \Delta\omega/\omega$, $\epsilon = 0$ corresponding to solid-body rotation. $\epsilon > 0$ means that the inner cylinder rotates in the same direction as the vessel but faster; in analogy with the meteorological practice, the counter-clockwise rotation of the vessel is called cyclonic, so in the case $\epsilon > 0$ we have anticyclonic shearing vorticity: $\partial\bar{v}/\partial r < 0$ ($\bar{v}$ being the zonal component of relative motion $\bar{\mathbf{v}}$). In the case $\epsilon < 0$ the inner cylinder rotates either in the same direction as the vessel but slower or into the opposite direction; in this case we have cyclonic shearing vorticity: $\partial\bar{v}/\partial r > 0$. The following five experiments corresponding to special values of the parameter ϵ were chosen as examples.

Experiment 1. $\epsilon = 0{\cdot}33$ ($\omega' = 4{\cdot}18\,\mathrm{s}^{-1}$, $\omega = 3{\cdot}14\,\mathrm{s}^{-1}$), see figures 3(*a*)–(*d*) (plate 2), taken 15, 60, 180 and 300 s after the start of rotation of the inner cylinder respectively.

Experiment 2. $\epsilon = 4$ ($\omega' = 2{\cdot}6\,\mathrm{s}^{-1}$, $\omega = 0{\cdot}52\,\mathrm{s}^{-1}$), see figures 4(*a*)–(*e*) (plate 3), taken 25, 50, 80, 105 and 160 s after the start of rotation of the inner cylinder respectively.

Experiment 3. $\epsilon = -0{\cdot}5$ ($\omega' = +1{\cdot}57\,\mathrm{s}^{-1}$, $\omega = +3{\cdot}14\,\mathrm{s}^{-1}$), see figures 5(*a*) and (*b*) (plate 4), taken 60 s and 13 min after the start of rotation of the inner cylinder respectively.

Experiment 4. $\epsilon = -2$ ($\omega' = -3{\cdot}14\,\mathrm{s}^{-1}$, $\omega = 3{\cdot}14\,\mathrm{s}^{-1}$), see figures 6(*a*)–(*c*) (plate 4), taken 20, 40 and 60 s after the start of rotation of the inner cylinder respectively.

Experiment 5. $\epsilon = 1{\cdot}5$ ($\omega' = 2{\cdot}6\,\mathrm{s}^{-1}$, $\omega = 1{\cdot}04\,\mathrm{s}^{-1}$), see figures 7(*a*)–(*d*) (plate 5), taken 40, 80, 120 and 160 s after the start of rotation of the inner cylinder respectively.

In experiments 1–4 there was a free surface, whereas in experiment 5 the upper surface was rigid. The diameter of the inner cylinder was 10 cm in each experiment and the height of water 20 cm; the bottom of the vessel (polished steel) can be regarded as a relatively smooth plane. All photographs have been taken from the side, the coloured regions being reproduced by grey tones. The constriction appearing on some of the pictures in the upper half of the coloured region is caused by a reflexion at the parabolic water surface.

Experiment 2 is a good example for illustrating the gradual development of the mean field of motion in the friction zone, until the steady state is attained, this being characterized by the sharp separation between the coloured region ($\bar{\mathbf{v}} \neq 0$) and the uncoloured region ($\bar{\mathbf{v}} = 0$).

4. Experimental results

Evaluating the data from the five experiments mentioned above in connexion with that of the other experiments yields the following results.

4.1. *The friction zone*

For both $\epsilon \lesseqgtr 0$ a field of relative motion exists in a steady state only within a limited region around the inner cylinder, the so-called friction zone, which in general shows axial symmetry, thus being independent of the zonal direction, and is sharply separated from the outer region, where no relative motion can be observed. For each value of $|\epsilon|$ the radial extent of the friction zone for $\epsilon > 0$ (anticyclonic shear) is greater than for $\epsilon < 0$ (cyclonic shear); the difference is approximately 15 % ($\pm$ 5 %). For comparison it may be mentioned here that in the case $\omega = 0$ ($\epsilon = \infty$) no limited region exists at all, on the contrary, throughout the vessel we observe a steady three-dimensional motion.

As our experiments have shown, the radial extent b of the friction zone can be regarded as a function of $\epsilon = \Delta\omega/\omega$ and the radius a of the inner cylinder: $b = F(\epsilon, a)$; the influence of the roughness at the bottom turns out to be of minor importance. Figure 8 shows the measured values for b plotted against the corresponding values of ϵ for $a = 5$ cm (measured values denoted by circles) and for $a = 12{\cdot}5$ cm (measured values marked by triangles). The individual values of $\Delta\omega$ and ω in these experiments have been chosen independently of one another, with $0 < n_1 \leqslant 30$, $0 < n_2 \leqslant 55$ r.p.m. ($\epsilon = \Delta\omega/\omega = (n_2 - n_1)/n_1$). The fact that we can get the same value of ϵ with different pairs $(\Delta\omega, \omega)$ has been used to examine the validity of the results for b. The experiments have been performed under

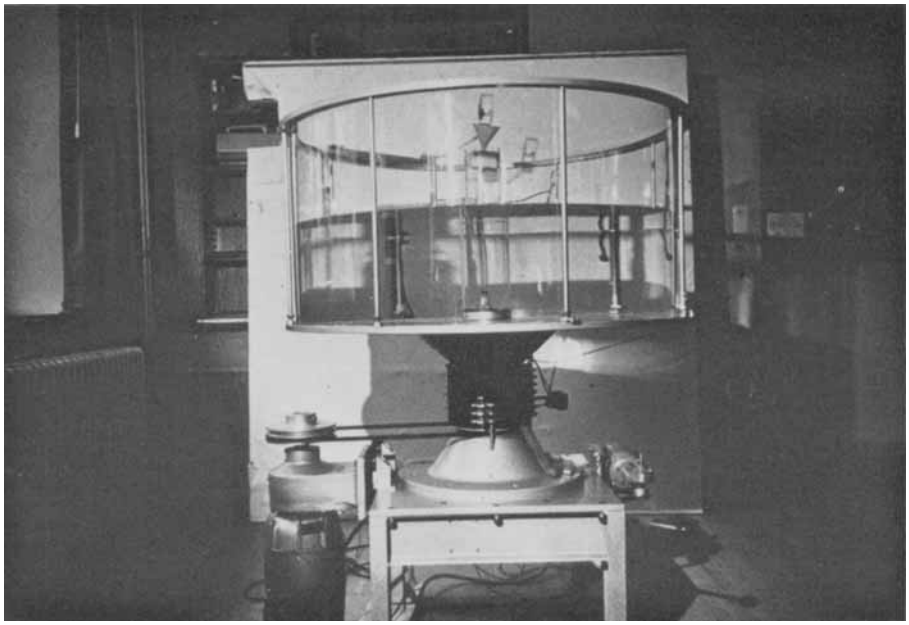

FIGURE 1. The model apparatus.

(*a*)

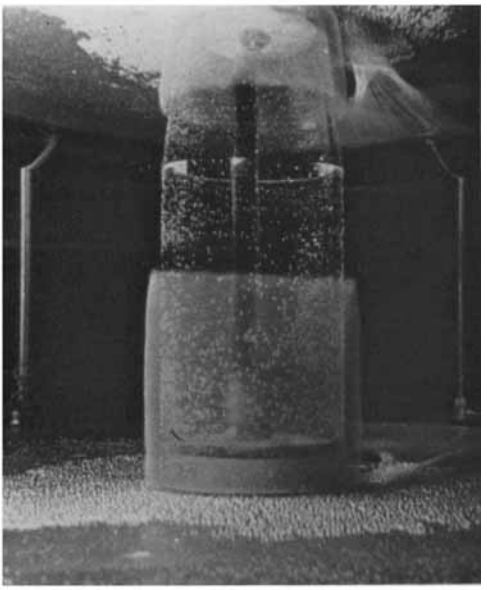

(*b*)

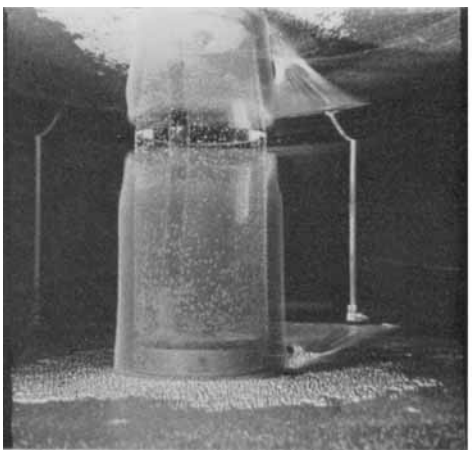

(*c*)

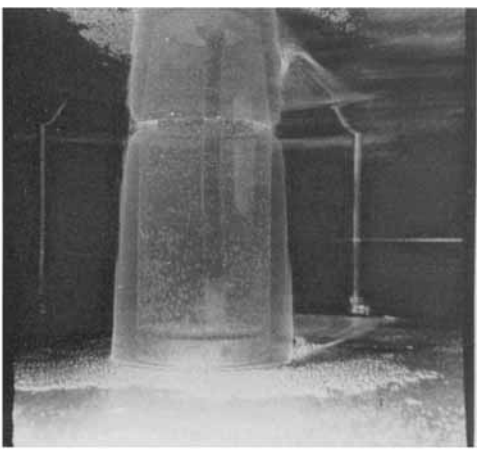

(*d*)

FIGURE 3. Experiment 1. $\epsilon = 0{\cdot}33$ ($\omega' = 4{\cdot}18\ \mathrm{s}^{-1}$, $\omega = 3{\cdot}14\ \mathrm{s}^{-1}$); free surface. Time after the start of rotation of the inner cylinder (relative rotation): (*a*) 15 s, (*b*) 60 s, (*c*) 180 s, (*d*) 300 s.

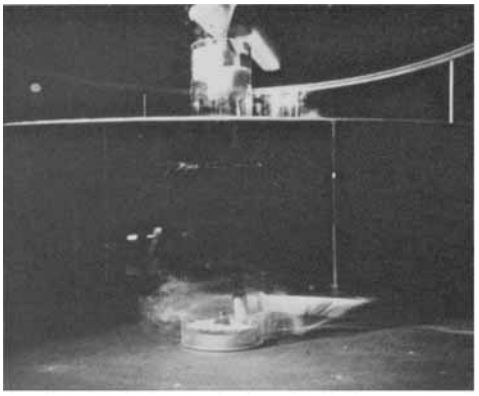

(*a*)

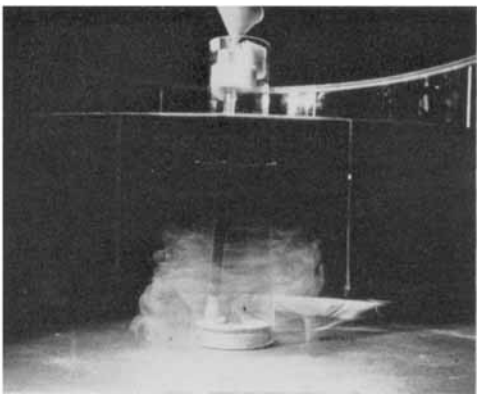

(*b*)

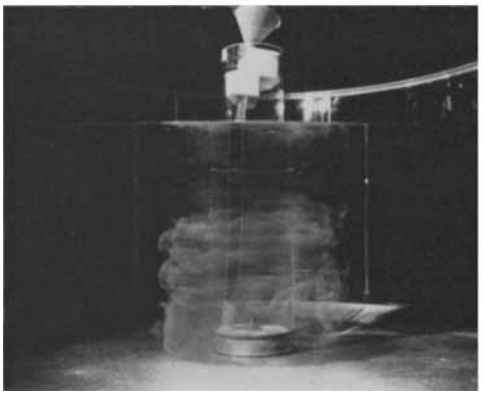

(*c*)

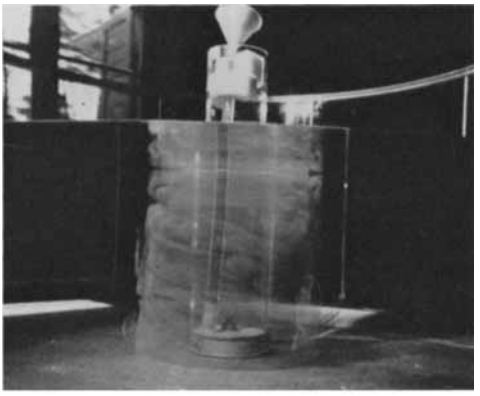

(*d*)

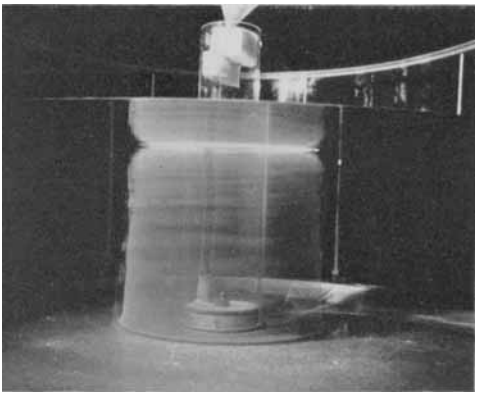

(*e*)

FIGURE 4. Experiment 2. $\epsilon = 4$ ($\omega' = 2{\cdot}6\ \mathrm{s}^{-1}$, $\omega = 0{\cdot}52\ \mathrm{s}^{-1}$); free surface. Time after the start of relative rotation: (*a*) 25 s, (*b*) 50 s, (*c*) 80 s, (*d*) 105 s, (*e*) 160 s.

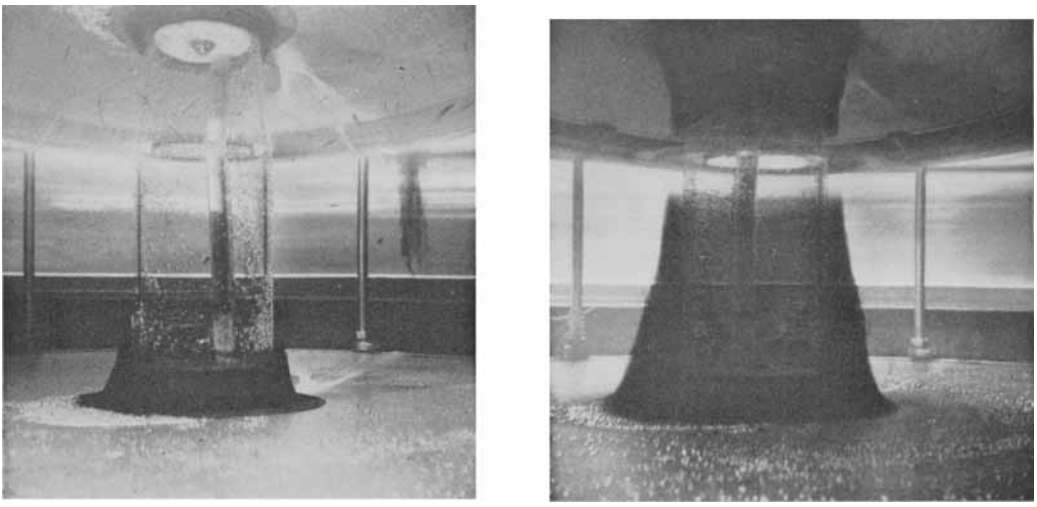

(*a*) (*b*)

FIGURE 5. Experiment 3. $\epsilon = -0{\cdot}5$ ($\omega' = 1{\cdot}57\ \mathrm{s}^{-1}$, $\omega = 3{\cdot}14\ \mathrm{s}^{-1}$); free surface. Time after the start of relative rotation: (*a*) 60 s, (*b*) 13 min.

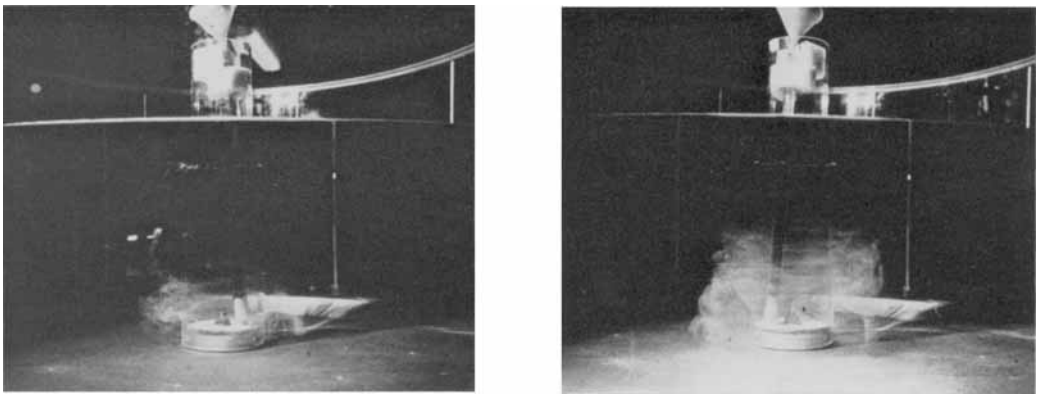

(*a*) (*b*)

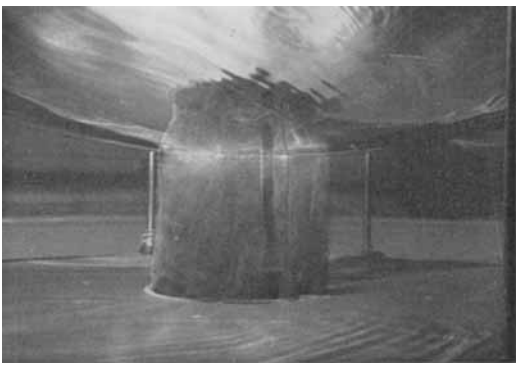

(*c*)

FIGURE 6. Experiment 4. $\epsilon = -2$ ($\omega' = -3{\cdot}14\ \mathrm{s}^{-1}$, $\omega = 3{\cdot}14\ \mathrm{s}^{-1}$); free surface. Time after the start of relative rotation: (*a*) 20 s, (*b*) 40 s, (*c*) 60 s.

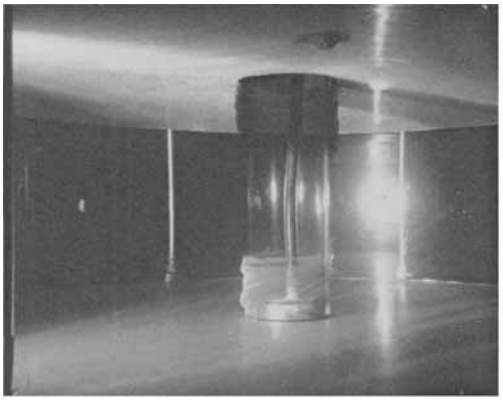

(*a*)

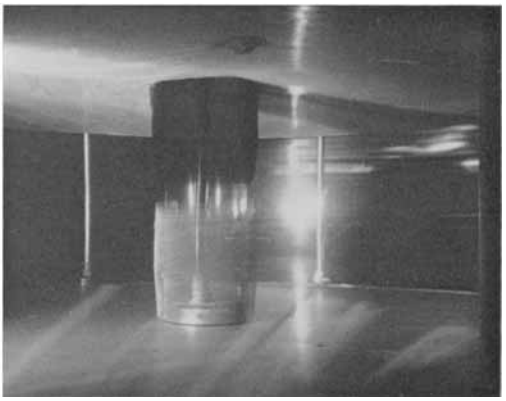

(*b*)

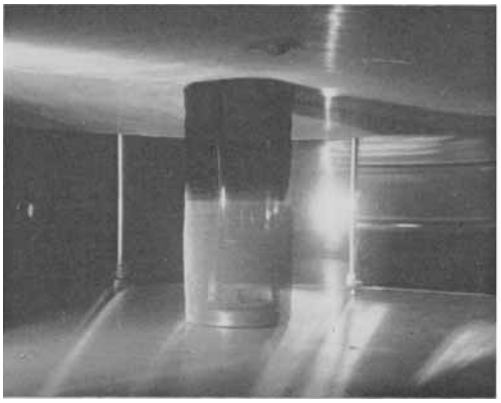

(*c*)

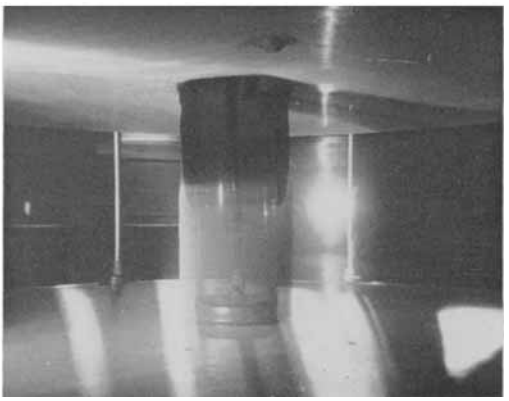

(*d*)

FIGURE 7. Experiment 5. $\epsilon = 1{\cdot}5$ ($\omega' = 2{\cdot}6$ s^{-1}, $\omega = 1{\cdot}04$ s^{-1}); rigid upper boundary. Time after the start of relative rotation: (*a*) 40 s, (*b*) 80 s, (*c*) 120 s, (*d*) 160 s.

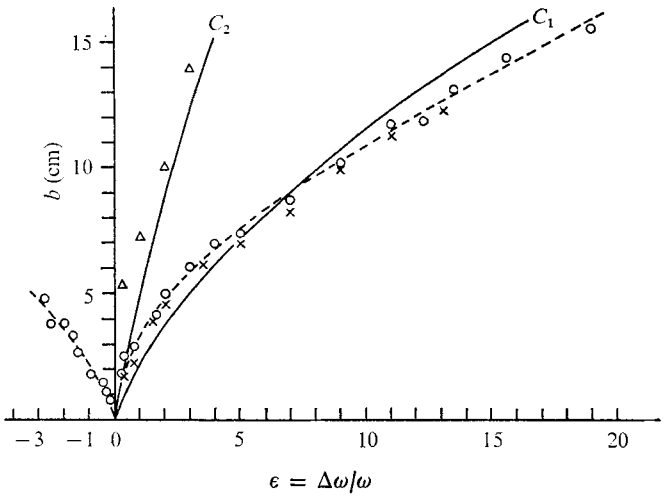

FIGURE 8. Radial extent b of the 'friction' zone as a function of ϵ. C_1, C_2, theoretical curves. Experimental values: ○, $a = 5$ cm, standard conditions; ×, $a = 5$ cm, increased roughness at bottom; △, $a = 12{\cdot}5$ cm, standard conditions.

'standard' conditions: free upper surface, height of water = 20 cm, the wall of the inner cylinder as well as the bottom of the vessel being relatively smooth. The points in figure 8 denoted by a cross represent values of b measured for increased roughness at the bottom and for $a = 5$ cm, other conditions being the same. The emery paper used in these experiments as a rough bottom layer has about 150 grains per cm^2, the grain size being 0·6–1·0 mm.

According to our findings the continuous supply of angular momentum at the inner cylinder, for the case $\epsilon > 0$, must be balanced by a continuous transport of momentum down to the bottom within the friction zone in order to guarantee the steady state. In the case $\epsilon < 0$ the direction of the transport processes is reversed: the momentum flux up from the bottom (because of its faster rotation compared with the flow) has now to be compensated by a transport towards the inner cylinder to achieve the steady state.

4.2. *The field of motion*

In general we can say that for both $\epsilon \gtrless 0$ the zonal velocity component $\bar{v}$ dominates the motion; by considering the absolute values we find that from the inner cylinder up to the outer limit of the friction zone it decreases monotonically. On average the radial velocity component $\bar{u}$ and the vertical velocity component $\bar{w}$ are about one to two orders of magnitude smaller than $\bar{v}$, constituting a weak mean 'meridional' circulation within the friction zone (see figure 2(*a*), where $\epsilon > 0$). The flow structure expresses a strong tendency to be two-dimensional. We now consider several cases in more detail.

The case $\epsilon > 0$. Close to the bottom, within a thin boundary layer, there exists a rather strong inward flow (with radial component $\bar{u}$) with a maximum of $\bar{u}$ near the inner cylinder; here the vertical component $\bar{w}$ also has its maximum, which is situated in the last 2–3 cm above the bottom. In the remaining upper

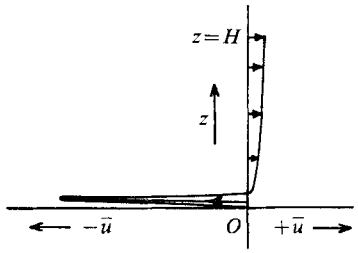

FIGURE 9. Vertical profile of the radial velocity component $\bar{u}$ at a point near the inner cylinder (schematic) for $\epsilon > 0$. A negative value corresponds to inward flow towards the centre and a positive value to outward flow; H = height of the upper surface.

region we find a compensating weak outward flow. Figure 9 represents schematically the vertical profile of the radial velocity component $\bar{u}$ near the inner cylinder; the relation $\int_0^H \bar{u}\,dz = 0$ should be satisfied (H = height of the surface).

Now, for small values of ϵ the mean meridional circulation $(\bar{u}, \bar{w})$ is well pronounced, turbulent mixing being rather weak; the development of the coloured friction zone, i.e. the distribution of the injected dye by the flow, happens rather slowly (see experiment 1, figure 3). For greater values of ϵ turbulent mixing becomes more and more significant and the mean circulation $(\bar{u}, \bar{w})$ cannot be easily identified. Now the development of the coloured friction zone proceeds much faster than is the case for small values of ϵ (see experiment 2, figure 4). The change from the flow structure revealed by experiment 1 to that found in experiment 2 takes place continuously, there is no sudden transition.

The case $-1 \leqslant \epsilon < 0$. In this case the mean meridional circulation, which is well pronounced, is reversed; near the bottom we have a rather strong outward flow, whereas the compensating flow in the upper region is now directed towards the centre. For the distribution of the injected dye by the flow much more time is necessary than in the case $\epsilon > 0$ (see experiment 3, figure 5).

The case $\epsilon < -1$. In contrast to the case $-1 \leqslant \epsilon < 0$, turbulent mixing now dominates the development of the coloured friction zone; close to the inner cylinder we observe a small area with wavy disturbances, which perturb the axial symmetry of the friction zone. Its radial extent b is now measured as a mean value (see experiment 4, figure 6).

5. Discussion

5.1. *The budget of absolute angular momentum*

The case $\epsilon > 0$. Here the inner cylinder must be regarded as a source of angular momentum. If we introduce a cylindrical co-ordinate system (r, ϕ, z) (for its orientation see figures 10(*a*) and (*b*)) and divide the velocity vector $\mathbf{v}$ (relative motion) into a mean part $\bar{\mathbf{v}} = (\bar{u}, \bar{v}, \bar{w})$ (the bar denoting the time average and $\bar{u}$ the radial, $\bar{v}$ the zonal and $\bar{w}$ the vertical velocity component) and a turbulent part $\mathbf{v}' = (u', v', w')$ for which $\overline{\mathbf{v}'} = 0$, then the equation for the absolute angular

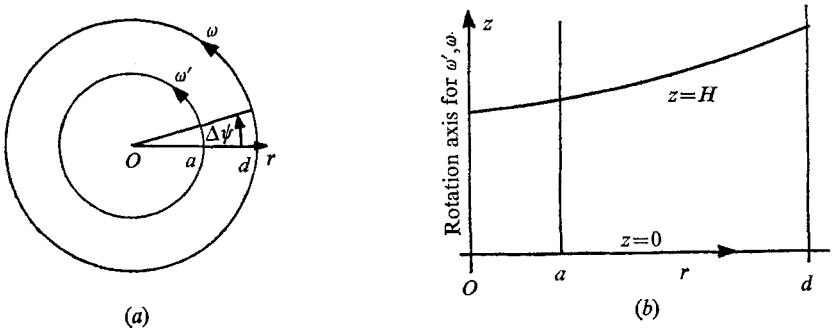

FIGURE 10. Orientation of the cylindrical co-ordinate system (r, ϕ, z). d is the radius of the vessel and ω its angular velocity; a is the radius of the inner cylinder and ω' its angular velocity; H = height of the free surface.

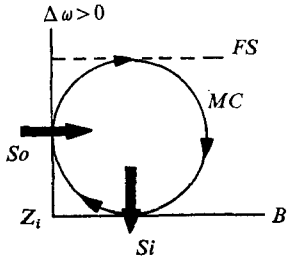

FIGURE 11. Angular momentum flux for $\epsilon > 0$ $(\Delta\omega > 0)$ with a free surface. Z_i is the inner cylinder, acting as a source (So) of angular momentum, B the rigid boundary (bottom of the vessel), representing a sink (Si) of momentum. Heavy arrows denote the direction of momentum transport, MC the mean 'meridional' circulation and FS the free surface.

momentum M_a per unit mass may be written, provided that there is rotational symmetry $(\partial/r\,\partial\phi = 0)$, as

$$\frac{\partial M_a}{\partial t}+\frac{1}{r}\frac{\partial}{\partial r}(r\bar{u}M_a)+\frac{1}{r}\frac{\partial}{\partial r}(r^2\overline{u'v'})+\frac{\partial}{\partial z}(\bar{w}M_a)+\frac{\partial}{\partial z}(r\overline{w'v'}) = 0; \tag{1}$$

$$\frac{1}{r}\frac{\partial}{\partial r}(r\bar{u})+\frac{\partial}{\partial z}\bar{w} = 0. \tag{2}$$

The absolute angular momentum per unit mass M_a refers to the vertical axis of rotation and is defined by $M_a = r\bar{v}+\omega r^2$.

Based upon a detailed analysis of the experimental results, the following conclusions may be drawn from equation (1).

(*a*) In the steady state $(\partial M_a/\partial t = 0)$ the mean and turbulent radial fluxes of angular momentum on the whole equal the vertical fluxes.

(*b*) To achieve the corresponding distribution of angular momentum both a turbulent exchange and a mean 'meridional' circulation $(\bar{u}, \bar{w})$ in the r, z plane are necessary (see figure 11).

(*c*) The influence of ω essentially becomes effective through the mean fluxes, which, compared with the turbulent fluxes, are more pronounced with increasing

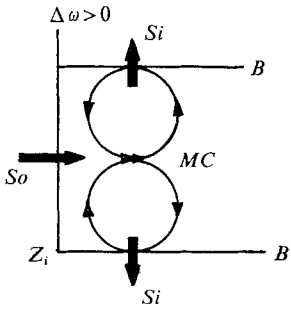

FIGURE 12

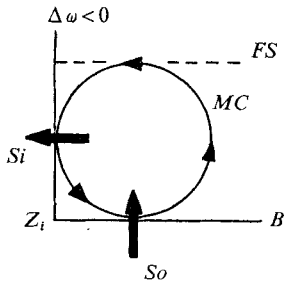

FIGURE 13

FIGURE 12. Angular momentum flux for $\epsilon > 0$ ($\Delta\omega > 0$) with a rigid upper boundary. Z_i is the inner cylinder, a source of angular momentum (*So*), B the rigid boundaries (bottom and rigid surface), representing sinks (*Si*) of momentum. Heavy arrows give the sense of momentum transport and *MC* is the mean 'meridional' circulation.

FIGURE 13. Angular momentum flux for $\epsilon < 0$ ($\Delta\omega < 0$) with a free surface. B is the rigid boundary (bottom), acting as a source (*So*) of angular momentum, Z_i the inner cylinder, representing a sink (*Si*) of momentum. Heavy arrows mark the direction of momentum flux, *MC* is the mean 'meridional' circulation and *FS* the free surface.

ω (smaller values of ϵ). If ω decreases to zero, the turbulent fluxes become more and more dominant; the friction zone will spread out, its radial extent b tending to infinity.

Experiment 5 (see figures 7 (*a*)–(*d*)) may illustrate these statements in a special case. If we have a rigid upper surface exerting an additional stress on the water the flux of angular momentum will follow the scheme represented in figure 12. In this case we may expect two meridional circulations. By colouring the two cells with different agents, we can see that for smaller values of ϵ ($0 < \epsilon < 1{\cdot}5$) both cells are preserved as 'individuals' for a certain time, turbulent mixing being rather weak. For greater values of ϵ, however, the mean structure of the cells becomes perturbed by increasing turbulent mixing.

The case $\epsilon < 0$. The considerations made in the case $\epsilon > 0$ can be transmitted to the case $\epsilon < 0$ if only the direction of the processes, the 'sign', are reversed; at the inner cylinder there is now a sink of angular momentum, whereas at the bottom we have a source. Figure 13 displays the corresponding momentum flux, the sense of the meridional circulation being reversed in this case.

5.2. *Inertial stability*

Now we have to answer the question why the field of motion $\bar{\mathbf{v}}$ remains limited to the friction zone, the radial extent of which for each value of $|\epsilon|$ depends upon whether ϵ takes positive or negative sign. Answering this question leads to a problem of inertial stability (Rayleigh 1917; Kleinschmidt 1941; Lin 1966). In the following we shall try an elementary approach to the problem.

The criterion for whether a state of motion is inertially stable or not is the increase of the absolute angular momentum $M_a = r\bar{v} + \omega r^2$ for increasing r, for which we may write

$$\frac{1}{r}\frac{\partial M_a}{\partial r} = \xi_a > 0, \tag{3}$$

where ξ_a is the absolute vorticity (axial symmetry).

The case $\epsilon > 0$. The observed flow structure admits the conclusion that to achieve the steady state the vertical momentum transports are necessary, but that the radial extension of the friction zone is essentially determined by the radial turbulent fluxes. In our rotating system it can be regarded as a problem of two-dimensional turbulent momentum exchange, in which the absolute angular momentum M_a is a conserved quantity.

The initial state of our experiments, the solid-body rotation, is inertially stable:

$$\xi_a = \frac{1}{r}\frac{\partial M_a}{\partial r} = 2\omega > 0.$$

Now, for $\epsilon > 0$ the inertial stability is weakened by the turbulent exchange, for the radial flux of angular momentum initiated by the rotating inner cylinder tries to eliminate the differences of absolute angular momentum and to establish a field of constant M_a within a certain area (a, r_0), i.e. the friction zone, with $a < r_0 < R$ (R = radius of the tank). At the outer limit r_0, which is to be determined, the zonal component $\bar{v}$ vanishes by definition: $\bar{v}(r_0) = 0$.

Now, according to our above considerations we can assume that for this area (a, r_0) the following equation is approximately valid:

$$M_a = r\bar{v} + \omega r^2 = C, \tag{4}$$

where C is a positive constant and $a \leqslant r \leqslant r_0$. At the inner cylinder ($r = a$) we have the boundary condition $\bar{v}(a) = a\Delta\omega$; for $r = r_0$ there is by definition $\bar{v}(r_0) = 0$.

By substituting $r = a$ and then $r = r_0$ into (4) and eliminating C, we obtain an equation for r_0:

$$\omega r_0^2 = a^2(\Delta\omega + \omega), \tag{5}$$

from which follows an expression for the radial extent $b = r_0 - a$ of the friction zone:

$$b = r_0 - a = a[(\epsilon+1)^{\frac{1}{2}} - 1], \quad \epsilon = \Delta\omega/\omega. \tag{6}$$

From (6) it follows that for $\epsilon \to \infty$, $(\omega \to 0)$, $b \to \infty$, i.e. no friction zone will exist in the case $\omega = 0$, as has already been mentioned above. The values of b calculated from (6) are in good agreement with the measured values (see figure 8, curves C_1 and C_2).

The case $\epsilon < 0$. Now the inner cylinder is a sink of angular momentum, and we should distinguish between the cases $\epsilon < -1$ and $-1 \leqslant \epsilon < 0$. Whereas for the former there is an inertially unstable region near the inner cylinder, the behaviour resembling that for $\epsilon > 0$, the inertial stability in the case $-1 \leqslant \epsilon < 0$ is strengthened by the flux of angular momentum.

In looking for an elementary approach to the case $-1 \leqslant \epsilon < 0$ we have investigated the possibility that the exchange processes as a whole tend to establish a field of motion which can be characterized by constant absolute vorticity $\xi_a = C_0 = \alpha \times 2\omega$ $(\alpha > 1)$. Then an equation similar to (6) can be derived; but the fact that an adjustable parameter α occurs and that it is not clear whether or not α is independent of ϵ makes this equation less noteworthy, so we have made no use of it.

In order to get more insight into the whole physical mechanism and the flow structure, especially in the case $\epsilon < 0$, and to determine the field of motion $\bar{\mathbf{v}}$ and the pressure distribution, we have to consider the friction zone as an inhomogeneous boundary-value problem and use numerical methods for solving it. The solution of this boundary-value problem has been attacked by Hinrichsen (1972).

The author is indebted to Prof. G. Fischer and to Mr K. Hinrichsen for useful advice during the course of this investigation.

REFERENCES

BANNON, J. K. 1952 Weather systems associated with some occasions of severe turbulence at high altitude. *Meteorol. Mag.* **81**, 97–101.

DUNST, M. 1967 Modellexperimente über die seitliche Vermischung in den Scherungsfeldern des Jetstream. *Hamburger Geophys. Einzelschr.* **8**, 39–96.

HINRICHSEN, K. 1972 The friction zone as a boundary-value problem (in preparation).

KLEINSCHMIDT, E. 1941 Stabilitätstheorie des geostrophischen Windes. *Ann. Hydrogr. Mar. Metor.* **69**, 305–325.

LIN, C. C. 1966 *The Theory of Hydrodynamic Stability.* Cambridge University Press.

RAYLEIGH, LORD 1917 On the dynamics of revolving fluids. *Proc. Roy. Soc.* A **93**, 148–58. (See also *Scientific Papers*, vol. 6, pp. 447–53. Cambridge University Press.)

REITER, E. R. 1961 *Meteorologie der Strahlströme (Jetstreams).* Springer.

ROSSBY, C. G. 1947 On the distribution of angular velocity in gaseous envelopes under the influence of large-scale horizontal mixing processes. *Bull. Am. Meteor. Soc.* **28**, 55–68.